Published in final edited form as:
J Am Chem Soc. 2011 April 20; 133(15): 5966–5975. doi:10.1021/ja111131f.

Quorum sensing between *Pseudomonas aeruginosa* biofilms accelerates cell growth

Shane T. Flickinger[a], **Matthew F. Copeland**[a], **Eric M. Downes**[a], **Andrew T. Braasch**[a], **Hannah H. Tuson**[a], **Ye-Jin Eun**[a], and **Douglas B. Weibel**[*,a,b]

[a]Department of Biochemistry, University of Wisconsin-Madison, Madison, WI 53706 U.S.A

[b]Department of Biomedical Engineering, University of Wisconsin-Madison, Madison, WI 53706 U.S.A

Abstract

This manuscript describes the fabrication of arrays of spatially confined chambers embossed in a layer of poly(ethylene glycol) diacrylate (PEGDA) and their application to studying quorum sensing between communities of *Pseudomonas aeruginosa*. We hypothesized that biofilms may produce stable chemical signaling gradients in close proximity to surfaces, which influence the growth and development of nearby microcolonies into biofilms. To test this hypothesis we embossed a layer of PEGDA with 1.5-mm wide chambers in which *P. aeruginosa* biofilms grew, secreted homoserine lactones (HSLs, small molecule regulators of quorum sensing), and formed spatial and temporal gradients of these compounds. In static growth conditions (i.e. no flow), nascent biofilms secreted *N*-(3-oxododecanoyl) HSL that formed a gradient in the hydrogel and was detected by *P. aeruginosa* cells that were ≤ 8 mm away. Diffusing HSLs increased the growth rate of cells in communities that were < 3 mm away from the biofilm, where the concentration of HSL was > 1 μM, and had little effect on communities farther away. The HSL gradient had no observable influence on biofilm structure. Surprisingly, 0.1–10 μM of *N*-(3-oxododecanoyl) HSL had no effect on cell growth in liquid culture. The results suggest that the secretion of HSLs from a biofilm enhances the growth of neighboring cells in contact with surfaces into communities and may influence their composition, organization, and diversity.

Introduction

Microbiology is historically colored by the mindset of bacteria as individual organisms. However, bacteria adhere and grow on nearly all surfaces and materials and form communities that are characterized by populations of cells encased in an extracellular polymeric substance.[1–4] It is widely believed that these communities—referred to as biofilms—are the dominant lifestyle of bacteria in the biosphere.[5] Biofilms provide cells with benefits that are not available to individual bacteria, including: (1) increased resistance to antibiotics;[6] (2) protection against predation by protozoa;[7,8] and (3) protection against host immune defenses.[9] The adherence of bacteria and their growth into biofilms on a wide-range of surfaces impacts ecology,[10] medicine,[11,12] and industry.[13,14] The significant financial and human health incentives associated with the eradication of biofilms has

Corresponding author: University of Wisconsin-Madison, Department of Biochemistry, 433 Babcock Drive, 471 Biochemistry Addition, Phone: +1 (608) 890-1342, Fax: +1 (608) 265-0764, weibel@biochem.wisc.edu.

Supporting Information Available: Experimental details; calculation of the HSL diffusion coefficient; and graphs and figures. Complete citation for Ref. [50]. This material is available free of charge via the Internet at http://pubs.acs.org.

stimulated studies investigating their mechanisms of formation and development, and techniques for their prevention and removal.[15]

The Gram-negative bacterium *Pseudomonas aeruginosa* is a model organism for studying biofilm formation.[16] Interest in *P. aeruginosa* biofilms has emerged in response to the prevalence of this organism and its status as a clinically important, opportunistic pathogen that infects hosts with compromised immune systems. The formation of *P. aeruginosa* biofilms and the accompanying increase in resistance of the cells to antimicrobial therapy, causes acute and chronic infections in individuals with cystic fibrosis.[17–19] *P. aeruginosa* biofilms form via a series of stages that include: (1) reversible attachment to a surface; (2) irreversible attachment; (3) microcolony formation; (4) biofilm maturation; and (5) dispersal.[20,21] The differentiation of planktonic *P. aeruginosa* cells into biofilms is cued by the production, secretion, diffusion, and sensing of chemical signals in a process referred to as quorum sensing (QS).[22–26] QS is a mechanism of regulated gene expression in bacterial communities in response to other cells and the physical constraints imposed by their environment.[27–30] The production of secondary metabolites activates transcription factors, which modulate the expression of QS target genes and coordinate gene expression across communities of cells. Some bacteria possess several interactive QS circuits, often under positive feedback control or autoinduction.[31,32] This process enhances the coordinated expression of QS target genes and results in population-wide phenotypes. QS is a mechanism that is involved in a variety of multicellular behaviors including biofilm formation,[33–36] virulence and pathogenicity,[12] motility, and swarming.[37]

The secretion and diffusion of secondary metabolites from bacterial communities has been qualitatively observed to influence the growth of adjacent communities.[38–41] QS signals appear to have a context-dependent influence on the development and structure of *P. aeruginosa* biofilms.[33,42–44] The extent to which gradients of QS signals secreted by communities regulate the formation and development of adjacent biofilms, and the length scale over which diffusing signals may influence other communities is not understood quantitatively. This phenomenon is particularly relevant to the developmental fate of microcolonies transforming into biofilms, which are in fluidic contact with adjacent communities and biofilms. We hypothesize that signaling molecules secreted from cells in microcolonies and biofilms may form gradients that persist for time scales in close proximity to surfaces that are long compared to gradients in three-dimensional liquid. Gradients may influence the growth and development of nearby communities into biofilms. In this manuscript we query this hypothesis using a polymer-based approach for controlling the length scale of chemical signaling between bacterial communities and its effect on cell growth and biofilm development. Using the QS circuit in *P. aeruginosa* as a model system, we demonstrate that nascent biofilms growing on surfaces produce a gradient of diffusing *N*-acyl homoserine lactones (HSLs) that enhances the growth of adjacent communities that are in close physical proximity.

Experimental Section

Fabrication of elastomeric stamps

We used a 1536-well microtiter plate with square wells as a master for creating poly(dimethylsiloxane) (PDMS) stamps (Figure 1F, inset); the dimensions of the chambers were 1.5 mm (wide), 5 mm (deep), with a pitch of 1.9 mm and a chamber wall thickness of 0.6 mm. A PDMS jig was placed in conformal contact with the surface of the plate. Wells inside the jig were filled with PDMS pre-polymer (10:1, base:curing agent) degassed under vacuum. PDMS was polymerized at 65 °C overnight and cured PDMS stamps were peeled away from the master. PDMS stamps were also prepared by replica molding techniques

using a pattern of SU-8 2050 photoresist in bas-relief on a silicon wafer master.[45] The resulting stamps had cylindrical posts that were 500-μm tall and 500-μm in diameter.

Fabrication of poly(ethylene glycol) diacrylate (PEGDA) hydrogel substrates

We used a method for fabricating PEGDA gels that is similar to the approach described by Tsutsui et al.[46] Briefly, we oxidized a PDMS stamp for 2 – 4 min in a plasma cleaner and immediately brought it into conformal contact with a silanized cover slip presenting acrylate groups (described in Supporting Information). A solution of poly(ethylene glycol) diacrylate (PEGDA) prepolymer solution (15% v/v) admixed with 2,2-dimethoxy-2-phenyl-acetophenone (5.8 mM) was introduced around the stamp and polymerized using a Dymax PC-3 UV light welder (λ320–395 nm, 4000 mW/cm^2, 150 s). We removed the PDMS stamp and soaked the hydrogel in sterile ddH_2O overnight to extract un-polymerized monomers and unbound oligomers. Prior to inoculation with bacteria, hydrogels were sterilized in a laminar flowhood by exposure to UV light for 2 – 3 h.

Construction of *P. aeruginosa* strains and growth conditions

We used several strains of *P. aeruginosa* in this study (Table 1). Details of the construction of PAO1-derived strains and the growth conditions for all *P. aeruginosa* strains are presented in Supporting Information. To grow biofilms in mesostructured gels, we inoculated individual chambers in a layer of PEGDA with a suspension of bacteria; the inoculate volume was smaller than the chamber volume. We found it difficult to inoculate individual PEGDA chambers with microscale dimensions. Therefore, we grew biofilms in microstructured chambers by submerging the embossed PEGDA in a suspension of bacteria.

Microscopy

A description of the protocols and materials for epifluorescence, environmental scanning electron (ESEM), and confocal laser scanning microscopy (CLSM) are found in Supporting Information.

Diffusion of HSLs produced by *P. aeruginosa* through PEGDA hydrogels

We placed a PDMS jig around a 15% PEGDA hydrogel embossed with a square array consisting of 36 chambers and removed the liquid culture media from the chambers. 10 μL of M8 media was added to the four center chambers in the array; the composition of M8 media is described in detail in the supporting information. We inoculated the remaining 32 chambers with a 10-μL aliquot of a dilute culture of *P. aeruginosa* PAO1 in M8 media (absorbance 0.2 at λ = 600 nm). A small volume of M8 media filled the space inside the jig to keep the gel hydrated. The gel was placed in a Petri dish and incubated at 37 °C for 24 h. The M8 media was removed from the four center chambers and replaced with 10 μL of a PAO-MW1 pUM15 subculture (absorbance 0.5 at λ = 600 nm) in Luria-Bertani (LB) broth. The gel was incubated an additional 10 h at 37 °C and YFP fluorescence was imaged in the chambers. As a positive control, we inoculated subcultures of PAO-MW1 pUM15 in LB (absorbance 0.5 at λ = 600 nm) admixed with 10 μM *N*-(3-oxododecanoyl) homoserine lactone (3O-C_{12}-HSL)—to activate YFP expression—in all 36 chambers of the array. We repeated the experiment without adding exogenous 3O-C_{12}-HSL as a negative control. We incubated the gels at 37 °C for 10 h and imaged YFP fluorescence in each chamber.

Determining the influence of the position within the array on *P. aeruginosa* growth rates

We fabricated 15% PEGDA hydrogels embossed with a square array consisting of 81 chambers. After removing liquid from the chambers, an 8-μL aliquot of a diluted PAO-MW1 overnight culture in 1:1 LB:M8 (absorbance 0.2 at λ = 600 nm) was added to select chambers of the array (yellow squares, Fig. S4A); 8 μL of M8 media was added to the

remaining chambers. Gels were stored in a Petri dish placed inside a sealable Ziploc bag lined with wet paper towels and incubated for 6, 12, 24, and 48 h at 37 °C. After incubation, we used a micropipette to mix the contents of each chamber containing PAO-MW1 by pipetting up and down. We removed a 7-μL aliquot from each chamber and added it to 93 μL of 1× PBS in a 96-well microtiter plate. We measured the absorbance (λ, 595 nm) in each well using a Tecan Infinite F200 plate reader (Fig. S4B). The experiment was performed in duplicate with four technical replicates per hydrogel.

To measure the influence of the position of the chambers in the array on cell growth using epifluorescence microscopy, we set up another series of hydrogels using the method described above. In this experiment we inoculated select chambers with PAO-MW1 p67T1, which constitutively expresses the red fluorescent protein, d-Tomato. We incubated the chambers and measured the fluorescence in each chamber at 0, 3, 6, 12, 24, and 48 h using epifluorescence microscopy (Fig. S4C).

Determining the influence of HSL diffusion from a *P. aeruginosa* community on the growth rate of adjacent communities

We fabricated and prepared hydrogels containing a square array consisting of 81 chambers to determine whether communities located in the center of the array affected cell growth in adjacent chambers into communities via secretion and diffusion of HSLs. In these experiments we inoculated the center chamber with strain PAO1 at two different times relative to the inoculation of the remaining chambers: 1) PAO1 was inoculated simultaneously with the inoculation of the remaining chambers with PAO-MW1 p67T1; or 2) we inoculated PAO1 into the center chamber, incubated for 12 h to form a nascent biofilm, and subsequently inoculated the remaining chambers with PAO-MW1 p67T1 cells. We measured and quantified cell growth by imaging d-Tomato fluorescence at 0, 3, 6, 12, and 24 h using epifluorescence microscopy.

We also measured the effect of HSLs on PAO1 cell growth in liquid broth culture. Cell cultures of PAO1 were grown overnight to saturation and then diluted 1:100 in M8 media in wells of a 96-well microtiter plate. We added 3O-C_{12}-HSL to microtiter plate wells at concentrations of 0, 0.1, 1, and 10 μm and measured the absorbance (λ, 595 nm) of each well every 30 min for 18 – 20 h using a Tecan Infinite F200 plate reader. The plates were shaken using an orbital amplitude of 1 mm during incubation.

Determining the spatial and temporal influence of diffusing HSLs on *P. aeruginosa* quorum sensing

We fabricated 15% PEDGA hydrogels embossed with a square array consisting of 81 chambers and removed residual liquid from the chambers. PAO1 cells were inoculated in hydrogel chambers using two different approaches, described below.

1. Inoculation after growth of a nascent PAO1 biofilm. We introduced an 8-μL aliquot of a diluted PAO1 overnight culture in M8 media (absorbance 0.2 at λ = 600 nm) to the center chamber of the array; 4 μL of M8 media was added to chambers in the cardinal and diagonal directions, and 8 μL of M8 media was added to the remaining chambers. The gel was stored in a Petri dish placed inside a sealable Ziploc bag lined with wet paper towels and incubated for 12 h at 37 °C. An overnight culture of PAO-MW1 pUM15 was centrifuged (3000 rpm, 10 min) and the liquid was removed. The pellet of bacteria was suspended in LB media containing 300 μg/mL carbenicillin (the absorbance of the suspension was adjusted to 0.4 at λ, 600 nm). We introduced a 4-μL aliquot of the diluted suspension of PAO-MW1 pUM15 cells into the chambers in the cardinal and diagonal directions in the PEDGA gel. The

hydrogel was placed in the Ziploc bag, incubated at 37 °C, and YFP expression was quantified by epifluorescence microscopy at 3, 6, 12, 24, and 48 h.

2. Simultaneous inoculation. This method was similar except that PAO1 and PAO-MW1 pUM15 were inoculated in hydrogel chambers simultaneously.

Spatial and temporal influence of diffusible metabolites and its effect on cell growth and biofilm structure

We performed experiments using a protocol that was similar to the first technique described in the previous section, except the chambers were inoculated with PAO-MW1 p67T1 instead of PAO-MW1 pUM15. We measured the fluorescence of d-Tomato to quantify biofilm structural parameters on a Nikon C1 confocal microscope after 12, 24, and 48 h. Image analysis was performed with COMSTAT[47] and structural parameters were determined for communities located different distances from the center chamber containing the nascent PAO1 biofilm.

Results and Discussion

We used a materials-based approach to study the role of chemical signaling between adjacent microcolonies and its effect on biofilm growth and development. The technique is related to a method we reported recently for fabricating biofilm arrays using PDMS stencils. The PDMS stencil defines regions of bacterial adhesion on surfaces on which cells grow and develop into biofilms.[48] Biofilms grown in these devices are in indirect fluidic contact with adjacent communities during their growth, however chemical communication between biofilms is disrupted for two reasons: (1) the PDMS walls are relatively impermeable to hydrophilic small molecules secreted by cells in biofilms; and (2) chemical signals secreted by cells diffuse into the large volume of liquid culture media whether they are diluted, and are subsequently removed under fluid flow. The study of chemical communication and its effect on biofilm development is not possible using this platform. Furthermore, cells adsorb non-specifically on PDMS and may disperse into the bulk media and contaminate adjacent communities, thus complicating the analysis of experiments involving the parallel study of biofilms of different strains of bacteria.

We replaced the PDMS stencil with a layer of PEGDA. The PEGDA was embossed with chambers that defined regions where bacteria adhered to the surface of a glass cover slip where cells grew into biofilms. The resulting hydrogel layer provided compartments with a user-defined volume, shape, and chamber wall thickness for the growth of bacterial communities and biofilms that were in fluidic contact, but were physically isolated from each other by the polymer walls.[40,49] The embossed chambers provided a controlled and uniform growth environment for biofilms in a parallel, reproducible format; there was very little non-specific adsorption of cells to PEGDA surfaces. Small molecules diffused through the PEGDA walls, which made it possible to study the effects of secondary metabolites produced and secreted by a community on the growth and development of adjacent communities under uniform environmental conditions. This system ensured cell-cell communication between communities occurs via diffusion of signaling molecules and secondary metabolites and not from physical contact between cells or biofilms.

Choice of PEGDA as a biomaterial

Poly(ethylene glycol) and its derivatives are widely used as biocompatible materials for a variety of biological applications including drug encapsulation and anti-fouling surfaces.[50,51] We fabricated microchambers in hydrogels consisting of crosslinked PEGDA (~575 number-average molecular weight of polymer) for two reasons. 1) PEG can be incorporated into biocompatible gels that resist the adsorption of proteins and mammalian

cells and reduce the adhesion of bacteria.[46,52–54] This characteristic restricted biofilm development in embossed gels from the bottom of the chambers upward, as the polymer prevented attachment of cells on the walls and top surface of the hydrogel. Biofilms grown in these structures were therefore excellent mimics of freestanding biofilms grown on two-dimensional surfaces. 2) It is possible to control the physical properties of PEGDA gels using different ratios of PEG-acrylate and PEGDA monomers. The PEGDA monomer can be crosslinked to surfaces modified with an organosilane containing a terminal acrylate moiety, which covalently bonds the layer, prevents cells from migrating under the gel, and resists delamination of the polymer.

Fabrication of PEGDA hydrogels

We fabricated gels by polymerizing PEGDA prepolymer in contact with an acrylate-modified surface[55] using the soft lithographic technique of micromolding in capillaries to define the dimensions of chambers for biofilm growth;[45,56] Tsutsui et al. has described an identical approach to pattern mammalian cells.[46] In this paper, we use hydrogel structures with two different sets of dimensions: (1) microstructured gels (e.g. chambers ~500 μm in diameter and in height); and (2) mesostructured gels made by molding the square wells of a 1536-well microtiter plate into PDMS to create stamps with square posts which yielded chambers in the hydrogel that were 1.5-mm wide and 5-mm high with a chamber wall thickness of 0.6 mm (Fig. 1). The ease of hydrogel preparation made it possible to create any desired configuration of gel height and size, in addition to size, shape, and spacing of the chambers.

P. aeruginosa forms biofilms in chambers embossed in PEGDA

We tested whether micro- or mesoscopic chambers embossed in PEGDA hydrogels were suitable environments for microbial growth and biofilm formation using static conditions (i.e. no flow). We inoculated chambers embossed in 15% PEGDA with cultures of *P. aeruginosa* PAO1 and incubated them at 37 °C. We imaged biofilms by CLSM using *P. aeruginosa* PAO1 cells that constitutively expressed GFP (PAO1 pTDK-GFP)[57] or with wild type cells stained with FM 4–64 styryl membrane dye (Fig. 2). CLSM images revealed that cells grew into biofilms that had a shape and dimensions imposed by the chamber walls.

Diffusion of small molecules in PEGDA hydrogels

To study chemical communication between biofilms, the time scale for small molecules diffusing across the length of the hydrogel must be comparable to biofilm formation. To characterize the diffusion of small organic molecules through a PEGDA hydrogel we used fluorescein as a model solute. A 10 mM aqueous solution of fluorescein was added to a reservoir at one end of a layer of 15% PEGDA. Using epifluorescence microscopy to image the diffusion of fluorescein and fitting the data to Fick's Law (Eq. 1 in Supporting Information), we estimated the diffusion coefficient through PEGDA, D_{PEGDA} to be ~0.08 – 0.13 $mm^2\ min^{-1}$. Since the hydrogels are embossed with chambers filled with liquid, and therefore not a homogenous layer of gel, we used an adjusted value of D that accounts for the entire volume of PEGDA hydrogel that a solute can diffuse through,

$$D = D_{PEGDA} / f_{PEGDA} \quad \text{(Eq. 1)}$$

where f_{PEGDA} is the fraction of the hydrogel area consisting of PEGDA. As the volume of a chamber wall (e.g. ~4.5 mm^3) is significantly larger than the volume of a biofilm growing in a chamber (e.g. ~0.2 mm^3, assuming an average biofilm thickness of ~0.1 mm), we took the entire PEGDA volume into account in deriving Equation 1.

The center-to-center distance of chambers in a row or column was 1.9 mm and the distance along a diagonal axis was 2.7 mm. Using these distances and *D*, we calculated the approximate time for a small molecule to diffuse from the center chamber to another chamber in the gel using the equation:

$$t = x^2/4D \quad \text{(Eq. 2)}$$

The doubling time of *P. aeruginosa* PAO1 in M8 liquid media was 60 min (Fig. S3). Small molecules secreted by cells in biofilms diffused through the PEGDA and reached cells in an adjacent chamber within one doubling time. For the largest array of chambers we used in our experiments—a square array consisting of 81 chambers—the distance from the center chamber, containing a nascent biofilm secreting HSLs, to the farthest chamber was 10.8 mm. Diffusing HSL reached the farthest chambers in 117 – 168 min, which was equivalent to ~2 – 3 doubling times. Thus, these substrates are suitable for studying the effects of HSL diffusion on cell growth and biofilm formation in adjacent chambers.

The PAO-MW1 pUM15 QS circuit is activated by the diffusion of HSLs produced by wild type PAO1 biofilms growing in adjacent chambers

We used *P. aeruginosa* to study the diffusion of native QS signaling molecules between biofilms. *P. aeruginosa* has two well characterized QS circuits centered upon the *lasRI* and *rhlRI* genes.[31,32] The proteins LasR and RhlR are members of the LuxR family of transcriptional regulators and bind 3O-C_{12}-HSL and *N*-butanoyl homoserine lactone (C_4-HSL), respectively (Fig. 3). LasI and RhlI synthesize HSLs. These two QS circuits are organized as a hierarchy with the *lasRI* system at the top, providing positive feedback to itself and to *rhlRI*.

As a pilot experiment, we used two strains of *P. aeruginosa*: wild type strain PAO1, and a Δ*lasI*/Δ*rhlI* mutant, PAO-MW1 pUM15.[58] Strain PAO-MW1 pUM15 contains a plasmid with the gene encoding yellow fluorescent protein (YFP) fused down stream of the promoter region of *rsa*L, which is expressed upon transcriptional regulation by HSL-bound LasR. PAO-MW1 pUM15 does not synthesize 3O-C_{12}-HSL; however it does have a functional LasR receptor. Thus, YFP is only expressed in the presence of exogenous 3O-C_{12}-HSL. We determined whether the QS circuit in PAO-MW1 pUM15 cells incubated in chambers could be activated by the diffusion of 3O-C_{12}-HSL synthesized by PAO1 biofilms in adjacent chambers. The readout for activation in our assay was the fluorescence of expressed YFP.

The experimental system consisted of a square array consisting of 36 chambers embossed in PEGDA (Fig. 4a). The four center chambers were filled with M8 media; the remaining 32 chambers were inoculated with PAO1 in M8 (Fig. 4b). We incubated gels for 24 h at 37 °C, removed M8 media from the four center chambers, and inoculated them with PAO-MW1 pUM15 in LB. After incubating the gels for 10 h at 37 °C, we quantified YFP expression using epifluorescence microscopy and image analysis (Fig. 4c). We found that only the four center chambers inoculated with PAO-MW1 pUM15 expressed YFP (Fig. 4d). The average fluorescence intensity of the four center chambers containing PAO-MW1 pUM15 was 407.3 ± 43.0, compared to 0.0 ± 0.2 for the outer wells (Fig. 4e). As PAO-MW1 pUM15 does not produce 3O-C_{12}-HSL and is physically isolated from PAO1 by the PEGDA chamber walls, it only produces YFP if 3O-C_{12}-HSL is synthesized by PAO1 in adjacent chambers and diffuses through the hydrogel. The expression of YFP provides evidence that bacterial communities can communicate chemically through PEGDA gels. As a positive control we inoculated all of the chambers with PAO-MW1 pUM15 in culture media containing exogenous 3O-C_{12}-HSL (10 μM). The mean fluorescent intensity of the chambers was 2856 ± 410 fluorescence units (Fig. S9). As the YFP fluorescence intensity of the positive control

was significantly higher than the data in our pilot experiments, we created a dose-response curve to correlate YFP fluorescence intensity with HSL concentration (Fig S10). The dose-response curve suggests that the concentration of 3O-C_{12}-HSL in the four center chambers after 10 h was ≤ 10 μM.

Determining the influence of HSLs on *P. aeruginosa* growth rates

Before investigating the spatial influence of diffusible 3O-C_{12}-HSL produced by biofilms grown in the hydrogel chambers, we determined whether the position of a chamber in the array had any effect on the growth rate of the cells within. Hypothetically, all chambers should provide equivalent environments; however chambers at the edge of the array have fewer neighbors than chambers in the center, which may influence the growth rate due to the local concentration of nutrients and metabolic waste. We fabricated a square array consisting of 81 chambers in PEGDA, inoculated the chambers with PAO-MW1 or PAO-MW1 p67T1, and determined cell growth by measuring absorbance (Fig. S4b) or d-Tomato fluorescence (Fig. S4b). We found that the rate of cell growth was identical at all positions in the hydrogel array.

To test whether 3O-C_{12}-HSL affects the growth rate of *P. aeruginosa*, we measured the growth curve of PAO1 in the presence of 0, 0.1, 1, and 10 μM 3O-C_{12}-HSL in a 96-well microtiter plate (Fig S3). 3O-C_{12}-HSL had no effect on growth rate; it did, however influence the density of cells at stationary phase. We investigated the effects of HSLs on *P. aeruginosa* cell growth rate in hydrogel chambers by constructing an 81-chamber hydrogel array and employing two different methods which varied the time at which wild type PAO1 cells—producing HSLs—were introduced in the center chamber (Fig S5a). PAO1 was either inoculated simultaneously with PAO-MW1 p67T1, such that there was no HSL gradient that PAO-MW1 p67T1 could detect, or a nascent PAO1 biofilm was formed in a chamber for 12 h before PAO-MW1 p67T1 cells were inoculated in adjacent chambers. We measured cell growth by d-Tomato fluorescence at 0, 3, 6, 12, and 24 h using fluorescence microscopy.

When PAO1 and PAO-MW1 p67T1 were inoculated simultaneously, cell growth in all chambers proceeded normally: the distance from the center chamber (containing PAO1) had no effect on cell growth of PAO-MW1 p67T1 (Fig. S5b). When PAO-MW1 p67T1 cells were inoculated in the chambers of a hydrogel array containing a nascent PAO1 biofilm, we observed that the growth rate of cells decreased as their distance from the biofilm increased (Fig. S5c and Fig. 5e). This result contrasts with our observation that the concentration of 3O-C_{12}-HSL does not influence the growth rate of PAO1 in liquid suspension, and suggests that the effect of this class of compounds is context dependent. The influence of 3O-C_{12}-HSL on cell growth rate in hydrogel chambers decreased linearly to ~8 mm from the center chamber after which cell growth rates between chambers were similar (Fig. S5c). To ensure that the increase in d-Tomato fluorescence was due to the influence of HSLs on growth and not an effect on the constitutive expression of d-Tomato, we measured the production of this fluorescent protein in the presence or absence of HSLs. 3O-C_{12}-HSL had no effect on d-Tomato expression (Fig. S6). The increase in the growth rate of *P. aeruginosa* in chambers proximal to the nascent biofilm is therefore due to sensing a gradient of HSLs produced by the biofilm growing in contact with the surface.

Determining the spatial and temporal influence of HSL diffusion from a nascent *P. aeruginosa* PAO1 biofilm on adjacent communities

Biofilms may influence the growth and organization of neighboring bacterial communities.[39–41] Inspired by these observations, we used PEGDA chambers to study the spatial and temporal influence of a nascent biofilm (12 h growth) on bacterial communities that are growing in close proximity (e.g. within a 10-mm radius). We introduced PAO1 into

the center chamber of a square array consisting of 81 chambers embossed in PEGDA (Fig. 5a). After incubating for 12 h at 37 °C, we inoculated select chambers with PAO-MW1 pUM15 (Fig. 5b). We incubated the gel and quantified YFP expression using epifluorescence microscopy (Fig. 5c). We found that YFP expressed by the communities increased to a maximum value of 500 fluorescence units between 24 – 48 h at a distance of 2.5 – 3 mm from the nascent PAO1 biofilm. YFP expression decreased linearly when the communities were ~3 – 8 mm in distance from the nascent PAO1 biofilm. Using a dose-response curve (Fig. S10) relating the concentration of 3O-C_{12}-HSL to the fluorescence intensity of expressed YFP at different times, we estimate that the concentration of 3O-C_{12}-HSL at communities positioned at a distance of 2.5 – 3 mm from the center chamber is ~1 μM (Fig. 5d). The concentration of 3O-C_{12}-HSL decreased linearly by 0.13 μM mm^{-1} to a distance of ~8 mm from the center chamber containing the PAO1 biofilm. In contrast, when we repeated the experiment by simultaneously inoculating chambers with PAO1 (center chamber) and PAO-MW1 pUM15 (remaining chambers) we only detected YFP expression in chambers closest to the center chamber; the fluorescence in the remaining chambers was below the sensitivity of our EMCCD camera (Fig. S7).

These results suggest that there is a potential relationship between the radius of the HSL gradient produced by a nascent biofilm and the growth rate of adjacent cells. Fig. 5e demonstrates the relationship between the position of microchambers and cell growth rates at 24 h, as measured by d-Tomato fluorescence (also plotted in Fig. S5c). The d-Tomato fluorescence data displays a trend similar to the YFP fluorescence. That is, the distance over which changes in growth occur (d-Tomato fluorescence) corresponds to the distance over which the response to HSLs occurs (YFP fluorescence). At 24 h, we observed that the maximal fluorescence response for cells was located 2.7-mm away from the PAO1 biofilm; beyond this distance, HSL sensing and cell growth decreased. The loss of a threshold level of HSL signal corresponds to the location in the PEGDA (~7.6-mm from the center) where we no longer observe an enhancement of cell growth. We confirmed the statistical significance of the d-Tomato data (in log base 10 form) by analyzing it using an ANOVA test and applying a Tukey's multiple comparison test of means. P-values for the comparison of d-tomato fluorescence in chambers at different pairs of distances are as follows: distances 1.9 and 7.6 mm, p=0.0002; distance 1.9 and 8.1 mm, p=0.009; distances 1.9 and 10.8 mm, p=0.0003; distances 2.7 and 7.6 mm, 0=0.0001; distances 2.7 and 8.1 mm, p=0.005; and distances 2.7 and 10.8 mm, p=0.0002.

Spatial and temporal influence of 3O-C_{12}-HSL on biofilm structure

To investigate the spatial effect of an HSL gradient produced by a nascent biofilm on the formation and structure of adjacent biofilms, we used an array of 81 chambers embossed in PEGDA. We grew a nascent biofilm of PAO1 in the center chamber for 12 h at 37 °C, inoculated select chambers with PAO-MW1 p67T1, and incubated the gel at 37 °C. As differences between fluorescence in adjacent chambers were small, and given the shape of the HSL gradient measured in our system, we found that the most meaningful comparisons were between measurements in the chambers that were closest ('inside', 2.7-mm from the center chamber) and farthest away ('outside', 10.7-mm from the center chamber) from the biofilm; we therefore adopted this convention for experiments in Figs 6. Using CLSM, we observed the formation of *P. aeruginosa* microcolonies on the floor of chambers at 12 h, nascent biofilms at 24 h, and the maturation of biofilms at 48 h (Fig 6). We observed that a nascent biofilm increases the growth rate of adjacent biofilms responding to the gradient of 3O-C_{12}-HSL (Fig. 5). Encouraged by this finding, we analyzed CLSM images of biofilms growing in the PEGDA chambers to determine whether there were quantitative structural differences in biofilms growing in different regions of the 3O-C_{12}-HSL gradient. We found

no statistically significant difference in biofilm roughness or thickness by COMSTAT[47] analysis after growth for 12 or 24 h (Fig. 6c).

Conclusions

This manuscript describes the study of the influence of diffusing secondary metabolites on *P. aeruginosa* cell growth and biofilm development. The PEGDA chambers provide a means of physically separating multiple bacterial strains or mutants of the same strain while maintaining fluidic/chemical contact. We demonstrate that nascent *P. aeruginosa* biofilms secrete HSLs, which form a concentration gradient and enhance the growth rate of biofilms in close proximity. We found a statistically significant difference in the growth rates of communities in close proximity to a nascent biofilm in contrast to those growing further away; these data were similar to the radius of the HSL gradient.

Interestingly, liquid cultures of *P. aeruginosa* growing in the presence of fluid shear were unaffected by a range of concentrations of HSL admixed in the culture media. In these conditions, biofilm formation proceeds very slowly, if at all, presumably because cells and communities are not attached to the surface. Thus, the influence of HSLs on biofilm growth suggests that the effect of these compounds on cells is context dependent. This observation supports the notion that QS may be the response of cells to a range of environmental factors including cell density, mass-transfer, molecular contact, and the spatial distribution of cells.[59] This response has been referred to as ‘efficiency sensing’. In theory, the presence of the HSL gradient negates the usual requirement for a ‘quorum’ and makes it possible for fewer planktonic cells to transition to life on a surface.

The spatial effect of the HSL gradient is surprisingly long-range and depends on the size of the nascent biofilm and the volume into which HSLs are secreted and diffuse. As all of these parameters are user-defined in this system, it should be possible to test how these variables affect cell growth and biofilm structure. The results of these experiments may lay the foundation for developing a theoretical framework describing the effect of the diffusion gradient on biofilm formation.

The limiting step in the diffusion of 3O-C_{12}-HSL in our experiments was the transport of molecules through the PEGDA hydrogel. Experiments using a different geometry (i.e. $\ell_{new} \neq \ell_{PEGDA}$) and/or material (i.e. $D_{new} \neq D_{PEGDA}$) will exhibit different rates of diffusion. Provided a change in the decay-rate of 3O-C_{12}-HSL does not compensate for a new geometry or material, the effective QS "calling distances" will also be altered. In a natural setting (e.g. open water), cell-cell interactions may change QS dynamics and diffusion will no longer be rate limiting for HSL transport, as the advection of molecules through water is faster than through the hydrogel. However, we do not expect the essentially "local" affect of 3O-C_{12}-HSL to change; cells that are close to an established community will be more strongly affected than cells further away. The experimental setup described in this manuscript should prove to be a useful tool for probing the dynamics of this relationship. Although PEGDA has not been described as a bacterial habitat, our measurement of the diffusion coefficient in a PEGDA hydrogel may still be relevant for the strains used in this study. For example, chronic *P. aeruginosa* infections of the lungs extend into the mucosal lining of the lung epithelium, which consists of a high viscosity polysaccharide gel through which HSLs may diffuse at rates that approach those we measured in PEGDA gels.

Recent observations suggest that the influence of HSLs on *P. aeruginosa* biofilm structure and development is context dependent.[33,42–44] It is therefore plausible that we would not observe differences in the structure of biofilms growing in different positions in the HSL gradient. We observed no difference in the structure of nascent biofilms growing at different

locations in the HSL gradient. Our observation is that the HSL gradient influences cell growth rates (Fig. 5) and not structure (Fig. 6). It is possible that differences in community structure and organization become more pronounced at later stages in biofilm formation. Additional experiments will make it possible to test this biofilm phenotype, and others, arising from growth in a gradient of HSLs. Gradients of secondary metabolites may both inhibit and promote the growth and development of nearby communities into biofilms and contribute to the genetic and phenotypic diversity of cells in these structures.

We envision that the technique described in this manuscript may be useful for studying a range of other biofilm phenomena, including: 1) mechanisms of chemical communication in bacterial communities, including inter- and intra-species chemical signaling pathways; 2) the stages of biofilm formation; 3) inhibition of QS; 4) cross talk among different species of bacteria and host-pathogen interactions; 5) the niche of each member of a ‘native’ multispecies biofilm; and 6) the development of strategies for biofilm control or therapeutic treatments.

Supplementary Material

Refer to Web version on PubMed Central for supplementary material.

Acknowledgments

We thank John Singer for *E. coli* HB101 p67T1, Peter Greenberg for *P. aeruginosa* PAO-MW1, Michelle Kielar for assistance with CLSM, Sarah Swanson for assistance with ESEM and CLSM performed at the Plant Imaging Center, Department of Botany, UW-Madison, Lars Renner for assistance with image analysis, and the Landick lab for use of their plate reader. We acknowledge a Searle Scholar Award, DARPA, 3M, DuPont, the Alfred P. Sloan Foundation, and the USDA (WIS01366) for funding in support of this research. This material is based upon work supported by the National Science Foundation under Grant No. DMR-0520527. M.F.C. is funded by an NIH biotechnology training grant (grant 5T32GM08349). H.H.T. is supported by an NIH National Research Service award (award T32 GM07215).

References

1. Costerton JW, Lewandowski Z, Caldwell DE, Korber DR, Lappin-Scott HM. Annu. Rev. Microbiol. 1995; 49:711. [PubMed: 8561477]
2. Donlan Rodney M. Emerg. Infect. Dis. 2002; 8:881. [PubMed: 12194761]
3. Kjelleberg, S.; Givskov, M., editors. The Biofilm Mode of Life: Mechanisms and Adaptations. 2007.
4. Lopez D, Vlamakis H, Kolter R. Cold Spring Harbor perspectives in biology. 2010; 2:a000398. [PubMed: 20519345]
5. Costerton JW, Geesey GG, Cheng KJ. Sci. Am. 1978; 238:86. [PubMed: 635520]
6. Mah TF, O'Toole GA. Trends Microbiol. 2001; 9:34. [PubMed: 11166241]
7. Matz C, Kjelleberg S. Trends Microbiol. 2005; 13:302. [PubMed: 15935676]
8. Matz C, Webb JS, Schupp PJ, Phang SY, Penesyan A, Egan S, Steinberg P, Kjelleberg S. Plos One. 2008; 3
9. Anderson GG, O'Toole GA. Curr. Top. Microbiol. Immunol. 2008; 322:85. [PubMed: 18453273]
10. Danhorn T, Fuqua C. Annu. Rev. Microbiol. 2007; 61:401. [PubMed: 17506679]
11. Bryers JD. Biotechnol. Bioeng. 2008; 100:1. [PubMed: 18366134]
12. Donlan RM, Costerton JW. Clin. Microbiol. Rev. 2002; 15:167. [PubMed: 11932229]
13. Coetser SE, Cloete TE. Crit. Rev. Microbiol. 2005; 31:213. [PubMed: 16417202]
14. Mattilasandholm T, Wirtanen G. Food Rev Int. 1992; 8:573.
15. Rosenhahn A, Schilp S, Kreuzer HJ, Grunze M. Phys Chem Chem Phys. 2010; 12:4275. [PubMed: 20407695]

16. Harmsen M, Yang LA, Pamp SJ, Tolker-Nielsen T. FEMS Immunol. Med. Microbiol. 2010; 59:253. [PubMed: 20497222]
17. Gomez MI, Prince A. Curr Opin Pharmacol. 2007; 7:244. [PubMed: 17418640]
18. Harrison F. Microbiology-(UK). 2007; 153:917.
19. Wagner VE, Iglewski BH. Clin. Rev. Allergy Immunol. 2008; 35:124. [PubMed: 18509765]
20. Monds RD, O'Toole GA. Trends Microbiol. 2009; 17:73. [PubMed: 19162483]
21. O'Toole G, Kaplan HB, Kolter R. Annu. Rev. Microbiol. 2000; 54:49. [PubMed: 11018124]
22. de Kievit TR. Environmental Microbiology. 2009; 11:279. [PubMed: 19196266]
23. Fuqua WC, Winans SC, Greenberg EP. J. Bacteriol. 1994; 176:269. [PubMed: 8288518]
24. Lazdunski AM, Ventre I, Sturgis JN. Nat Rev Microbiol. 2004; 2:581. [PubMed: 15197393]
25. Waters CM, Bassler BL. Annu. Rev. Cell Dev. Biol. 2005; 21:319. [PubMed: 16212498]
26. Jayaraman A, Wood TK. Annu Rev Biomed Eng. 2008; 10:145. [PubMed: 18647113]
27. Boedicker JQ, Vincent ME, Ismagilov RF. Angewandte Chemie, International Edition. 2009; 48:5908.
28. Carnes EC, Lopez DM, Donegan NP, Cheung A, Gresham H, Timmins GS, Brinker CJ. Nat Chem Biol. 2010; 6:41. [PubMed: 19935660]
29. Horswill AR, Stoodley P, Stewart PS, Parsek MR. Anal Bioanal Chem. 2007; 387:371. [PubMed: 17047948]
30. Redfield RJ. Trends Microbiol. 2002; 10:365. [PubMed: 12160634]
31. Venturi V. FEMS Microbiol. Rev. 2006; 30:274. [PubMed: 16472307]
32. Williams P, Camara M. Curr. Opin. Microbiol. 2009; 12:182. [PubMed: 19249239]
33. Davies DG, Parsek MR, Pearson JP, Iglewski BH, Costerton JW, Greenberg EP. Science. 1998; 280:295. [PubMed: 9535661]
34. Dobretsov S, Teplitski M, Paul V. Biofouling. 2009; 25:413. [PubMed: 19306145]
35. Kjelleberg S, Molin S. Curr. Opin. Microbiol. 2002; 5:254. [PubMed: 12057678]
36. Parsek MR, Greenberg EP. Trends Microbiol. 2005; 13:27. [PubMed: 15639629]
37. Daniels R, Vanderleyden J, Michiels J. FEMS Microbiol. Rev. 2004; 28:261. [PubMed: 15449604]
38. Brenner K, You LC, Arnold FH. Trends Biotechnol. 2008; 26:483. [PubMed: 18675483]
39. D'Onofrio A, Crawford JM, Stewart EJ, Witt K, Gavrish E, Epstein S, Clardy J, Lewis K. Chem. Biol. 2010; 17:254. [PubMed: 20338517]
40. Kim HJ, Boedicker JQ, Choi JW, Ismagilov RF. Proc. Natl. Acad. Sci. U. S. A. 2008; 105:18188. [PubMed: 19011107]
41. Gantner S, Schmid M, Durr C, Schuhegger R, Steidle A, Hutzler P, Langebartels C, Eberl L, Hartmann A, Dazzo FB. Fems Microbiol Ecol. 2006; 56:188. [PubMed: 16629749]
42. Brooun A, Liu S, Lewis K. Antimicrob. Agents Chemother. 2000; 44:640. [PubMed: 10681331]
43. Heydorn A, Ersboll B, Kato J, Hentzer M, Parsek MR, Tolker-Nielsen T, Givskov M, Molin S. Appl. Environ. Microbiol. 2002; 68:2008. [PubMed: 11916724]
44. Stoodley, P.; Jørgensen, F.; Williams, P.; Lappin-Scott, H. Biofilms: the good, the bad, and the ugly;. Bayston, R.; Brading, M.; Gilbert, P.; Walker, J.; Wimpenny, JWT., editors. Cardiff, UK: Bioline; 1999. p. 323
45. Weibel DB, DiLuzio WR, Whitesides GM. Nat Rev Microbiol. 2007; 5:209. [PubMed: 17304250]
46. Tsutsui, H.; Wu, H.; Ho, CM. The 10th International Conference on Miniaturized Systems for Chemistry and Life Sciences; Tokyo, Japan. 2006.
47. Heydorn A, Nielsen AT, Hentzer M, Sternberg C, Givskov M, Ersboll BK, Molin S. Microbiol-Uk. 2000; 146:2395.
48. Eun Y-J, Weibel DB. Langmuir. 2009; 25:4643. [PubMed: 19215108]
49. Kaeberlein T, Lewis K, Epstein SS. Science. 2002; 296:1127. [PubMed: 12004133]
50. Ekblad T, et al. Biomacromolecules. 2008; 9:2775. [PubMed: 18759475]
51. Lin CC, Anseth KS. Pharm. Res. 2009; 26:631. [PubMed: 19089601]
52. Koh WG, Revzin A, Simonian A, Reeves T, Pishko M. Biomed Microdevices. 2003; 5:11.
53. Krsko P, Kaplan JB, Libera M. Acta Biomater. 2009; 5:589. [PubMed: 18842467]

54. Lee JH, Kim HE, Im JH, Bae YM, Choi JS, Huh KM, Lee CS. Colloid Surface B. 2008; 64:126.
55. Revzin A, Russell RJ, Yadavalli VK, Koh W-G, Deister C, Hile DD, Mellott MB, Pishko MV. Langmuir. 2001; 17:5440. [PubMed: 12448421]
56. Kim E, Xia Y, Whitesides GM. Nature (London). 1995; 376:581.
57. De Kievit TR, Gillis R, Marx S, Brown C, Iglewski BH. Appl. Environ. Microbiol. 2001; 67:1865. [PubMed: 11282644]
58. Muh U, Schuster M, Heim R, Singh A, Olson ER, Greenberg EP. Antimicrob. Agents Chemother. 2006; 50:3674. [PubMed: 16966394]
59. Fuqua C, Parsek MR, Greenberg EP. Annu. Rev. Genet. 2001; 35:439. [PubMed: 11700290]
60. Holloway BW, Krishnapillai V, Morgan AF. Microbiol. Rev. 1979; 43:73. [PubMed: 111024]
61. Whiteley M, Lee KM, Greenberg EP. Proc. Natl. Acad. Sci. U. S. A. 1999; 96:13904. [PubMed: 10570171]

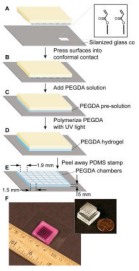

Figure 1.

Fabrication of structured PEGDA hydrogels. A) A cartoon of a PDMS stamp with square posts in bas-relief, and a glass cover slip derivatized with a silane presenting a terminal acrylate functional group. B) The PDMS stamp is pressed into conformal contact with the glass cover slip. C) A 15% PEGDA pre-polymer solution is added to the mold, filling the void spaces between the posts of the PDMS stamp. D) Exposure to UV light polymerizes the PEGDA. E) Peeling away the PDMS stamp reveals chambers embossed in a layer of hydrogel where the floor of the chamber is formed by the surface of the glass cover slip. Note that cartoons are not drawn to scale (see critical dimensions on the cartoon). F) An image of an array of 36 chambers (1-mm wide, 5-mm deep) embossed in a layer of 15% PEGDA hydrogel on a glass cover slip. The gel was stained with a red dye to enhance the details of the chambers for the image. Inset: An image of the PDMS stamp used to create the hydrogel.

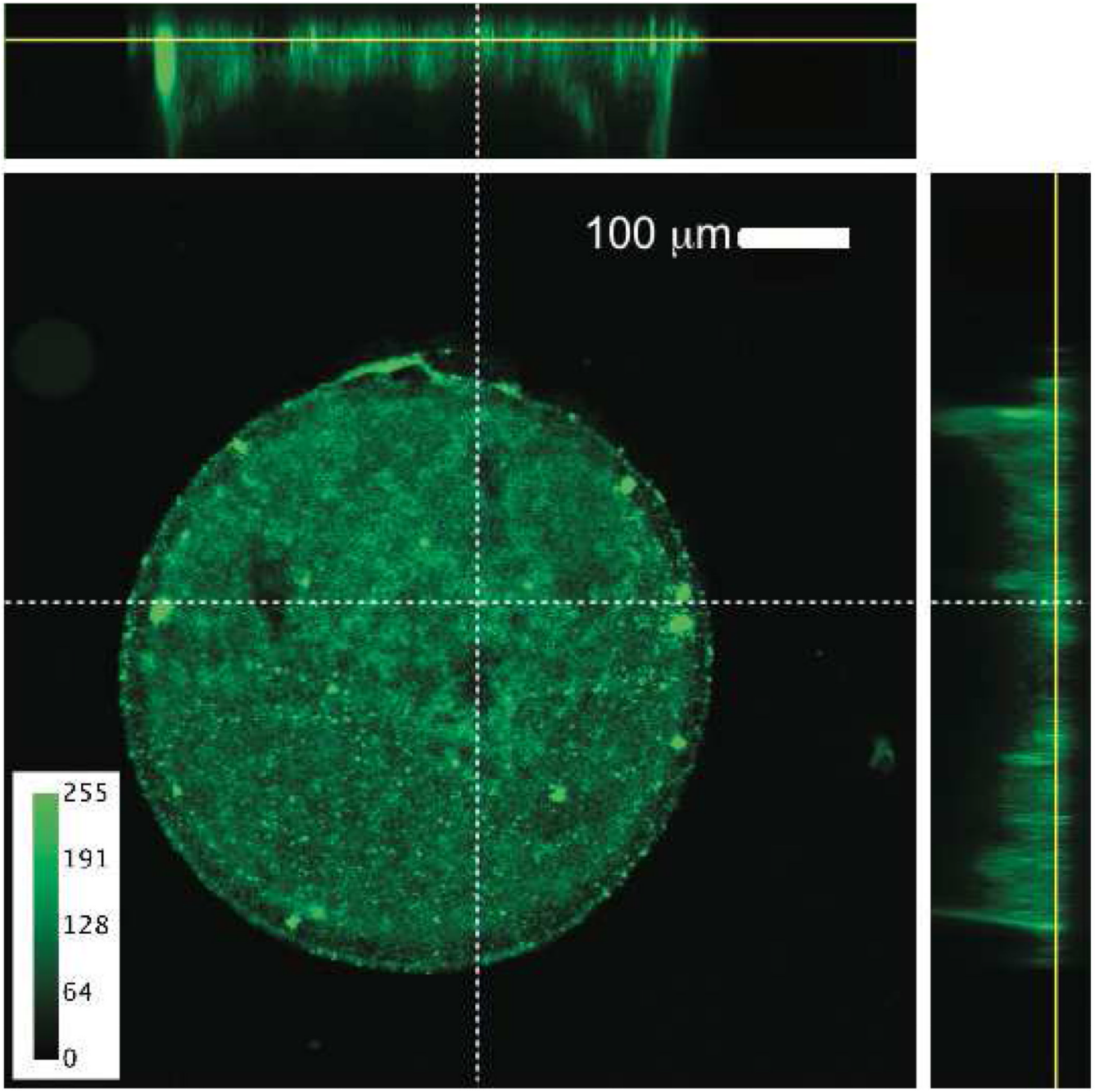

Figure 2.
CLSM image of a *P. aeruginosa* PAO1 biofilm after 72 h growing in a microchamber embossed in a layer of 15% PEGDA hydrogel. The biofilm was stained with FM 4–64 membrane dye. White dashed lines indicate the relative *x* or *y* coordinates of the orthogonal views, and the yellow line shows the coordinate along the *z*-axis.

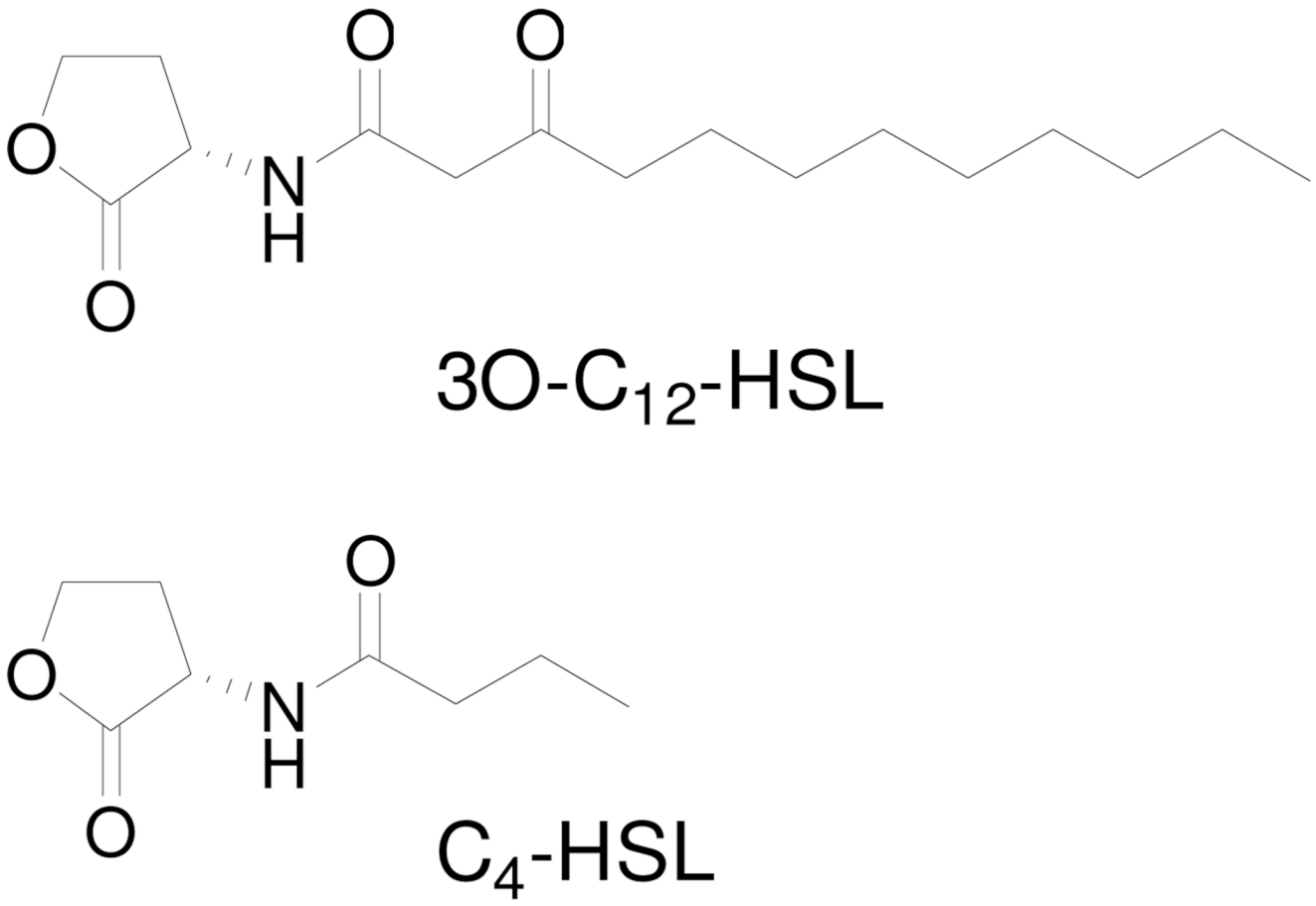

Figure 3.
Structures of N-acyl homoserine lactones that regulate quorum sensing in *P. aeruginosa*.

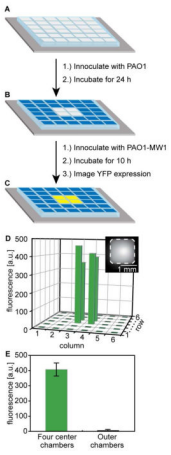

Figure 4.

The PAO-MW1 QS circuit is activated by the diffusion of HSLs produced by wild type PAO1 biofilms growing in adjacent chambers. A) The experimental system consisted of a 6 × 6 array of mesoscale chambers embossed in a 15% PEGDA hydrogel. B) The four center chambers were filled with M8 media and did not contain cells (white squares); the remaining 32 chambers were inoculated with PAO1 from a diluted overnight culture in M8 minimal media (blue squares). C) The gel was incubated for 24 h at 37 °C. The media in the four center chambers was removed and replaced with inoculates of PAO-MW1pUM15 sub-cultured in LB growth media (yellow squares). The hydrogel was incubated for 10 h at 37 °C and imaged to quantify YFP expression. D) A 3D-plot of YFP fluorescence in the 36-chamber array. Only the four center chambers containing PAO-MW1pUM15 expressed YFP activity relative to the outer wells inoculated with PAO1. Inset: Fluorescent image of one of the four center chambers containing PAO-MW1 pUM15. Scale bar = 0.5 mm. E) A plot of the average fluorescent intensity for chambers inoculated with PAO1 or PAO-MW1pUM15. The average fluorescent intensity for the four center chambers containing PAO-MW1 pUM15 was 407.3 ± 43.0; the intensity of the outer wells was 0.0 ± 0.2.

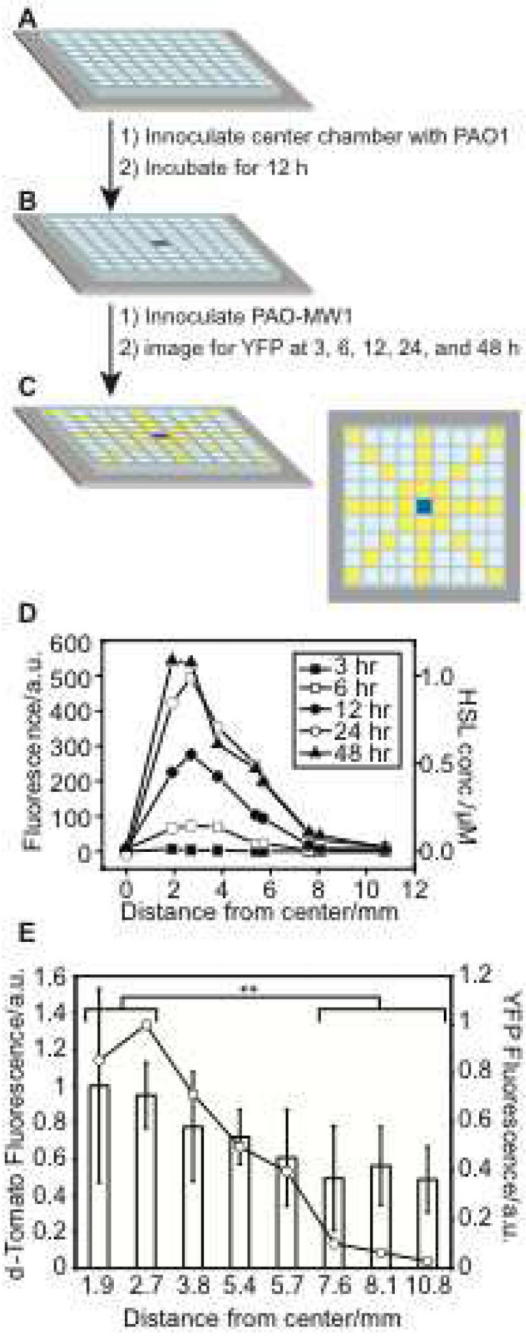

Figure 5.

Determining the spatial and temporal influence of diffusible metabolites produced by *P. aeruginosa* biofilms in proximity to developing *P. aeruginosa* communities. A) A cartoon of an array of 81 chambers embossed in PEGDA. B) The center chamber was inoculated with PAO1 from a diluted overnight culture in M8 (blue square); the remaining chambers were filled with M8 (white squares). C) The gel was incubated for 12 h at 37 °C and chambers in the cardinal and diagonal directions were inoculated with PAO-MW1 pUM15 (yellow squares) from a diluted overnight culture in LB. The gel was incubated at 37 °C and YFP expression was quantified by imaging after 3, 6, 12, 24, and 48 h. D) A plot of YFP fluorescent intensity in chambers containing PAO-MW1 pUM15 versus their distance

(center-to-center) from the center chamber containing PAO1 at different time intervals. E) A plot of d-Tomato fluorescence at 24 h (demonstrating cell density; bar graph) versus chamber distance overlaid with YFP fluorescence at 24 h (demonstrating response to the HSL gradient; open circles) versus chamber distance. Both sets of fluorescence data were normalized. The double asterisks indicates data points that had a p-value < 0.01; p-values are indicated in the text.

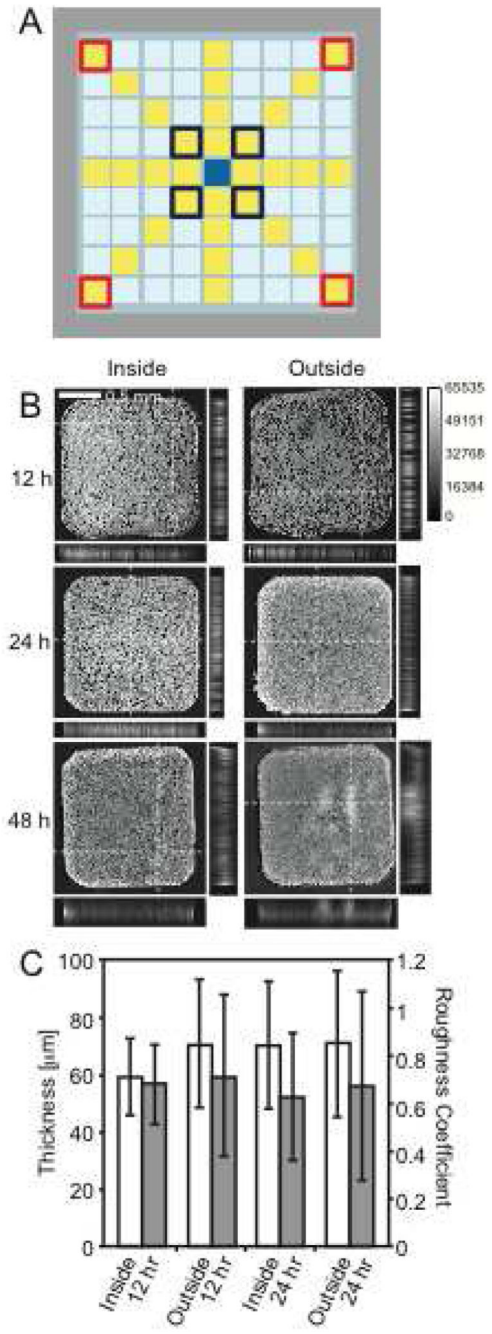

Figure 6.

Determining the influence of HSLs produced by wild type *P. aeruginosa* biofilms on the structure of developing *P. aeruginosa* biofilms. A) The cartoon depicts an array of 81 microchambers in PEGDA. The center chamber contains wild type PAO1 (blue square), and chambers along the cardinal and diagonal directions contain PAO-MW1 p67T1 (yellow squares). Remaining chambers contained M8 media (light blue squares). B) Three-dimensional reconstructions of biofilms from CLSM images and corresponding orthogonal views of a biofilm in an inside chamber (blue boxes in A) and an outside chamber (red boxes in A). White dashed lines indicate the relative *x* or *y* coordinates of the orthogonal views in the 3D reconstructions. Cells were fluorescent and appear white; regions of the

structure that are devoid of cells appear dark (e.g. at 12 h). The topography of the biofilm becomes visible at 48 h. C) A plot depicting COMSTAT analysis of biofilm thickness (white bars) and the coefficient of roughness (dark bars) at 12 hr and 24 hr.

Table 1

P. aeruginosa strains used in this study

Strain	Growth media	Phenotype	Reference
P. aeruginosa PAO1	LB agar/M8 media	wild type	60
P. aeruginosa pTdK-GFP	M8 with 200 μg/mL carbenicillin	expresses GFP (GFPmut3.1 gene under control of *lac* promoter; Amp^R)	57
P. aeruginosa PAO-MW1	LB	cannot produce HSLs (Δ*lasI*/Δ*rhlI*)	61
P. aeruginosa PAO-MW1 (pUM15)	LB with 300 μg/mL carbenicillin	cannot produce HSLs; produces YFP when QS circuit is activated in response to exogenous HSLs (Δ*lasI*/Δ*rhlI; rsaL* transcriptional fusion to *yfp*; Amp^R)	58
P. aeruginosa PAO-MW1 (p67T1)	LB with 300 μg/mL carbenicillin	cannot produce HSLs; expresses a form of RFP (Δ*lasI*/Δ*rhlI;* d-tomato constitutively expressed from plasmid, Amp^R)	this study
P. aeruginosa PAO1 (p67T1)	LB with 300 μg/mL carbenicillin	wild type constitutively expressing a form of RFP (d-tomato constitutively expressed from plasmid, Amp^R)	this study